HHS Public Access

Author manuscript

J Thorac Oncol. Author manuscript; available in PMC 2020 May 01.

Published in final edited form as:

J Thorac Oncol. 2019 May ; 14(5): 825–834. doi:10.1016/j.jtho.2018.12.003.

Expanding the Molecular Characterization of Thoracic Inflammatory Myofibroblastic Tumors beyond *ALK* gene rearrangements

Jason C Chang[1], **Lei Zhang**[1], **Alexander E Drilon**[2], **Ping Chi**[2,3,4], **Rita Alaggio**[5], **Laetitia Borsu**[1], **Ryma Benayed**[1], **William D Travis**[1], **Marc Ladanyi**[1,3], and **Cristina R Antonescu**[1,*]

[1]Department of Pathology, Memorial Sloan Kettering Cancer Center, New York, NY

[2]Department of Medicine, MSKCC, New York, NY

[3]Human Oncology and Pathogenesis Program, MSKCC, New York, NY

[4]Department of Medicine, Weill Cornell Medical College, New York, New York, USA

[5]Department of Pathology, University Pittsburgh Medical Center, Pittsburgh, PA

Abstract

Background: Half of inflammatory myofibroblastic tumors (IMTs) regardless of anatomic location harbor *ALK* gene rearrangements and overexpress ALK protein. The wide application of next generation sequencing (NGS) and the clinical benefit to tyrosine kinase inhibitors have opened new opportunities for investigation of ALK-negative IMT.

Design: In this study we investigate a series of pediatric and adult thoracic IMT for abnormalities in a wide spectrum of actionable kinases, by applying a variety of molecular and NGS techniques, including FISH, targeted RNA sequencing and NanoString.

Results: There were 33 thoracic IMTs, with a mean age of 37, including 5 children. Tumors showed a monomorphic spindle cell phenotype, except one with epithelioid morphology and moderate to severe atypia. By IHC, 24 cases were ALK positive, of which by FISH, 19 showed *ALK* rearrangements and 1 *RET* gene rearrangement. RNA sequencing was performed in the remaining 4 cases lacking *ALK* abnormalities by FISH, revealing *ALK* fusions in 3 cases, involving *TMP4* and *EML4* genes. NanoString was performed in the remaining case, revealing *ALK*-alternative transcription initiation (ALK^{ATI}). Nine cases lacking *ALK* abnormalities were further tested by FISH or targeted RNA sequencing, revealing *ROS1* rearrangement in 6 cases and *ETV6-NTRK3* fusion in 3, respectively.

*Correspondence to: Cristina R Antonescu, MD, Department of Pathology, Memorial Sloan Kettering Cancer Center, 1275 York Ave, New York, NY 10065 (antonesc@mskcc.org).

Conflict of interest: none

Conclusions: By employing a battery of complementary molecular techniques, all thoracic IMTs harbored a tyrosine kinase abnormality, with 30% outside the ALK kinase, including gene fusions involving *ROS1, NTRK3*, and *RET*. We also describe for the first time ALK^{ATI}-induced ALK oncogenic activation is involved in the pathogenesis of IMTs.

Keywords

inflammatory myofibroblastic tumor; ALK; ROS1; NTRK3; fusion; kinase

INTRODUCTION

IMTs display a wide morphologic spectrum, ranging from a predominantly inflammatory lesion with a paucity of spindle cells and prominent chronic inflammation and/or hyalinized stroma, to a highly cellular myofibroblastic proliferation and occasionally frankly sarcomatous neoplasm, lacking a significant inflammatory and/or stromal component. Due to its variable morphologic phenotype and lack of a consistent immunoprofile, the diagnosis of IMTs in the absence of *ALK*-rearrangements has been often a diagnosis of exclusion with a challenging differential diagnosis, including at one end of the spectrum reactive/inflammatory processes, such as sclerosing mediastinitis, fibro-inflammatory IgG4-related diseases[1], MALT lymphoma, and pulmonary hyalinizing granuloma, while at the other end of the spectrum, spindle cell sarcomas with myofibroblastic or fibroblastic features. Furthermore, ALK immunoreactivity, as an expression of *ALK*-based gene fusions, is more prevalent in pediatric IMT compared to the adult counterpart[2, 3]. However, it remains unclear if the discrepant prevalence of ALK abnormalities is an intrinsic variation in the IMT biology between the two age groups, or rather a reflection of the wider spectrum of lesions in adults that are classified under the broad term of IMT, which otherwise have no genetic relationship. The quest for a more definitive pathologic diagnosis and molecular characterization of locally aggressive or advanced/metastatic IMTs is quite critical as a number of FDA-approved kinase inhibitors are now available and can be used as targeted therapeutic strategies based on the specific genomic profile of these tumors. This study uses a number of sensitive and complementary molecular tools for gene fusion detection in a large cohort of thoracic IMTs diagnosed at our Institution in order to define alternative mechanisms of kinase activations beyond *ALK* fusions.

MATERIAL AND METHODS

Tumor Samples and Patient Information

Thirty-three cases of thoracic IMT were identified through retrospective search of clinical cases at Memorial Sloan Kettering Cancer Center (MSKCC) and from consultation files of the senior authors (CRA and WDT). The patients were 25 females and 8 males, with a median age of 37 (range: 2 to 75 years), including 5 pediatric patients. The anatomical sites, gross pathologic features, and patient outcomes were obtained from review of clinical notes and through discussion with pathologists and/or clinicians from the submitting institutions. Seven cases were previously included in a prior study[4]. The histologic slides were re-reviewed and the following morphologic features were recorded: tumor cell appearance (spindle, epithelioid), nuclear pleomorphism (mild, moderate), amount of inflammatory

infiltrate (abundant, scant), and mitotic activity. This study was approved by the institutional review board of MSKCC.

Immunohistochemistry (IHC).—Immunohistochemical antibodies for ALK (Cell Signaling; clone D5F3, pre-diluted), ROS1 (Cell Signaling; clone D4D6, 1:25), and pan-NTRK (Abcam; clone EPR17341, 1:166) were performed on cases with available material following standard procedures on either Ventana (Ventana Medical Systems, Tucson, AZ), DAKO (DAKO USA, Santa Clara, CA), or Leica-Bond-3 (Leica, Buffalo Grove, IL) automated instruments.

Fluorescence In Situ Hybridization (FISH).—FISH on interphase nuclei from paraffin-embedded 4-μm sections was performed using bacterial artificial chromosomes (BAC) custom probes, flanking genes of interest. The BAC clones were obtained from BACPAC sources of Children's Hospital of Oakland Research Institute (Oakland, CA; http://bacpac.chori.org). DNA from individual BACs was isolated according to the manufacturer's instructions, labeled with different fluorochromes in a nick translation reaction, denatured, and hybridized to pretreated slides. Slides were then incubated, washed, and mounted with DAPI in an antifade solution, as previously described[4]. The genomic location of each BAC set was verified by hybridizing them to normal metaphase chromosomes. Two hundred successive nuclei were examined using a Zeiss fluorescence microscope (Zeiss Axioplan, Oberkochen, Germany), controlled by Isis 5 software (Metasystems, Newton, MA). A positive score was interpreted when at least 20% of the nuclei showed a break-apart signal. Nuclei with incomplete set of signals were omitted from the score. All cases were tested for ALK gene rearrangements. Tumors lacking *ALK* gene abnormalities were further investigated by FISH for structural alterations in *ROS1, RET, PDGFRB*, and *NTRK3* genes using BACs previously published[4, 5]. *ALK*-rearranged tumors were further investigated for *EML4* gene abnormalities by FISH, *ROS1*-rearranged tumors were additionally tested for *TFG* alterations, and *NTRK3*-rearranged tumors were further tested for *ETV6* abnormalities.

Anchored Multiplex RNA Sequencing (Archer Dx)

For Anchored Multiplex RNA sequencing assay, the detailed procedure has been previously described[6]. Tumor samples lacking *ALK, ROS1, PDGFRB, NTRK3*, and *RET* rearrangements by FISH underwent targeted RNA sequencing to assess for gene fusions and other abnormalities that are not detectable by FISH. Unidirectional gene-specific primers were designed to target specific exons in 62 genes known to be involved in oncogenic fusions in solid tumors (Supplemental Table 1). In brief, RNA was extracted from formalin-fixed paraffin embedded (FFPE) specimens, followed by cDNA synthesis and library preparation. Anchored Multiplex polymerase chain reaction amplicons were sequenced on Illumina Miseq, and the data was analyzed using the Archer software.

NanoString Assay.—Details of the nCounter Analysis System (NanoString Technologies) were described previously[7, 8]. In brief, 9, 1, and 6 sequence-specific probes were constructed for ALK exons 1–19, intron 19, and exons 20–29, respectively. Five housekeeping genes (*OAZ1, PGK, RPS13, RPL27*, and *RPS20*) were used for RNA sample quality assessment and gene expression normalization. The probes were complementary to a 100 bp region of

the target mRNA (Supplemental Table 2). The raw data were normalized by successively subtracting the non-template control background and the positive control's geometric mean via the nSolver Analysis software, and the data were used to calculate fold-change in gene expression[9]. To be considered a positive sample, the expression ratios of the ALK intron 19 counts to the average housekeeping gene (R^{UTR}) should be greater than 0.5, and the expression ratios of the 3' ALK probes to the 5' ALK probes ($R^{3'vs5'}$) should be above 5.

RESULTS

Pathologic Findings

The specimens included biopsies (n=9), wedge resections (n=8), lobectomies (n=15), and pneumonectomy (n=1). Macroscopically, the tumors were well-circumscribed in all cases and involved the bronchial lumen in a subset of cases (n=10). The median gross tumor size was 2.3 cm (range: 1.0 to 15.4 cm).

Histologic, immunohistochemical, and molecular findings were summarized in Table 1. Morphologically, the tumors showed a variegated spectrum, ranging from spindled (n=27), mixed spindled and epithelioid (n=5), and pure epithelioid (n=1) in appearance. Architecturally, the tumors exhibited predominantly fascicular (n=17), mixed fascicular and storiform (n=14), and solid patterns (n=2). Cytologic atypia was typically mild to focally moderate, with only one case showing moderate to severe nuclear atypia. Mitotic activity ranged from 0 to 15 mitoses per 10 high power fields (hpf), with a median mitotic rate of 1 per 10 hpf. The nuclear features and mitotic counts were assessed using hpf at 400x magnification (0.237 mm^2 field of view) using an Olympus BX43 microscope (Olympus, Tokyo, Japan) with a standard eyepiece of 22mm diameter. Mitoses were evaluated in the 30 hpf areas with the highest mitotic activities and counted as an average of mitotic figures per 10 hpf (2.4 mm^2 area)[10]. The admixed inflammatory infiltrate ranged from scant (n=3) to moderate (n=7) to abundant (n=23). Necrosis was present in three cases.

ALK-positive IMTs show a high concordance with *ALK* gene abnormalities.

ALK-D5F3 IHC was performed on all 32 IMTs. With the exception of two cases that directly underwent RNA-sequencing, ALK-FISH was performed in the remaining 30 cases. Twenty-four of 33 cases (73%) were positive for ALK IHC. Of the 24 cases that showed ALK IHC positivity, 19 cases showed *ALK* rearrangement by FISH, and one case showed *RET* rearrangement by FISH. Targeted RNA sequencing was performed in the 4 cases lacking FISH abnormalities, revealing ALK fusions in 3 cases, involving *TMP4-ALK* (1 case) and *EML4-ALK* (2 cases). The last case lacking *ALK* abnormalities by FISH and targeted RNA sequencing underwent Nanostring testing, revealing ALK-alternative transcription initiation (ALK^{ATI}), as detailed below. ALK immunoreactivity showed a high concordance with the presence of *ALK* gene alterations, with a sensitivity of 100% and specificity of 85%.

One thoracic IMT harboring *ALK* rearrangement (IMT9) showed significant cytologic atypia, pure epithelioid morphology, and brisk mitotic activity (15 mitoses per 10 hpf) that raised the consideration of an alternative designation of epithelioid inflammatory fibroblastic

sarcoma (Supplemental Fig. 1A)[11]. The tumor occurred in a 70 year-old woman who presented with chest pain and dyspnea. A chest CT scan showed left pleural effusion with numerous pleural/fissural nodularities. Histologically, the tumors were composed of discohesive cells with eccentrically located nuclei, conspicuous nucleoli, and foamy cytoplasm arranged in solid and alveolar pattern, surrounded by moderately abundant myxoid stroma containing scant inflammation. The tumor cells were positive for ALK IHC (Supplemental Fig. 1B) and showed *ALK* rearrangement by FISH. Additional FISH studies were negative for *RANBP2* alterations.

Novel ALK^{ATI} Identified in one pulmonary IMT as a novel alternative mechanism of ALK activation

The lesion (IMT23) occurred in a 40-year-old man with history of low-grade follicular lymphoma presenting with cough, wheezing, and mild dyspnea. He was diagnosed with pneumonia and during hospitalization he underwent a bronchoscopy, which revealed an endobronchial mass involving the right bronchus intermedius. The tumor consisted of plump spindle cells with mild atypia arranged in a vague storiform pattern, admixed with a moderately abundant inflammatory infiltrate, typical of IMT (Fig. 1A). Although the tumor cells showed diffuse cytoplasmic immunoreactivity for ALK-D5F3 (Fig. 1B), subsequent FISH and RNA sequencing assays failed to demonstrate an ALK rearrangement. Due to the discrepant IHC and molecular results, the RNA sequencing data were manually reviewed, showing soft-clipped reads 5' to ALK exon 19 that raise the possibility of ALK^{ATI}. The finding was confirmed on NanoString assay, which is clinically validated for ALK^{ATI} detection, revealing a R^{UTR} of 0.73 and $R^{3'vs5'}$ of 65.6, confirming the presence of ALK^{ATI} (Fig. 1C). The patient underwent a therapeutic bronchoscopy that excised the residual tumor; another subsequent bronchoscopic debridement showed ulceration and granulation tissue with no residual tumor seen. The patient was free of disease at 3 months follow up.

Alternative non-ALK mechanisms of kinase activation include *ROS1, NTRK3*, and *RET* related fusions.

Two cases (IMT 29 and IMT32) that were negative for ALK IHC underwent targeted RNA sequencing directly, revealing *TFG-ROS1* and *ETV6-NTRK3* fusions, respectively. Eight cases lacking *ALK* gene abnormalities by FISH and molecular assays underwent additional FISH testing for *ROS1, PDGFRB, NTRK3*, and *RET*. Four cases showed *ROS1* gene rearrangements, 2 cases showed *NTRK3* rearrangements, and 1 case showed *RET* rearrangement. Three cases showing *ROS1* rearrangements by FISH were further examined with *TFG* probes and were negative for *TFG* alterations. One case lacking any FISH alterations in all kinase genes tested was subjected to targeted RNA sequencing, revealing a *TFG-ROS1* fusion.

Overall, 6 *ROS1*-rearranged thoracic IMTs were identified (see Table 1), two of which were reported previously[4]. Five tumors occurred in the lung and one in the mediastinum. There were 2 male and 4 female patients with a median age of 26 years (range, 4 to 75 years), including 3 children. Morphologically, most *ROS1*-rearranged tumors grew as solid, well-circumscribed nodules, while one tumor (IMT29) focally exhibited a peculiar interstitial pattern entrapping native alveolar parenchyma, mimicking a pseudotumor (Fig. 2A). All

ROS1-rearranged tumors were composed of spindle cells with tapered nuclei and distinctive slender cytoplasmic processes that were arranged in loose fascicles and embedded in a variably fibrous to fibromyxoid stroma containing moderate to abundant inflammatory infiltrate (Fig. 2B). All cases lacked significant cytologic atypia and showed low mitotic activity (1 per 10 hpf). All *ROS1*-rearranged IMTs were negative for ALK-D5F3 IHC. ROS1 IHC was performed in all cases, revealing diffuse cytoplasmic positivity in 3 (Fig. 2C), weak focal positivity in 2, and absence of staining in the last case. Both cases tested by RNA sequencing showed *TFG-ROS1* fusion (Fig. 2D). In one of these cases (IMT29), the diagnosis of IgG4-related disease was initially favored due to a moderately elevated IgG4/IgG ratio by immunohistochemistry and an exuberant lymphoplasmacytic infiltrate with very few spindle cells. However, the solitary lung nodule was the only site of disease, and there was no elevation of serum IgG4 levels. After discovery of the *ROS1* fusion by targeted RNA sequencing, ROS1 immunohistochemistry was performed revealing focal positive staining in myofibroblastic cells that was overlooked in the initial evaluation of the tumor. These myofibroblastic cells comprised less than 5% of the overall cellularity, which consisted of mostly lymphocytes and plasma cells.

Three cases showed the presence of *NTRK3* gene rearrangements by FISH (n=2) or targeted RNA sequencing (n=1). In the two cases with *NTRK3* gene rearrangements by FISH, further analysis using break-apart *ETV6* gene probes confirmed the presence of an *ETV6-NTRK3* fusion in both cases. One case (IMT32) occurred as an incidental 1.2 cm lung mass in a 2 year-old boy with a history of adrenal neuroblastoma and followed up with serial chest CT scans. Histologically, the tumor showed plump spindle cells with fascicular growth pattern surrounded by moderately abundant fibromyxoid stroma containing numerous psammomatous calcifications and abundant inflammatory cell infiltrate (Fig. 3A). The lesional cells were devoid of significant cytologic atypia and showed a low mitotic index less than 1 mitosis per 10 hpf. The second case (IMT31) occurred in a 31 year-old woman who presented with upper respiratory tract infection. She had an abnormal chest X-ray suggestive of a lung nodule, followed by a chest CT revealing a 1.8 cm well-circumscribed nodule in the right lower lobe. Histologically, the tumor was composed of plump spindle cells with short fascicular and vague storiform patterns embedded in abundant myxoid stroma containing marked chronic inflammation (Fig. 3B). The tumor cells lacked significant cytologic atypia and also showed low mitotic activity (1 mitosis per 10 hpf). The third case (IMT33) occurred in a 61 year-old woman undergoing chemotherapy and radiation for stage IV lung adenocarcinoma who had been followed up with serial CT scans, revealing a new growing 1.1 cm lung nodule. Histologically, the nodule showed a dense chronic inflammatory infiltrate consisting predominantly of plasma cells (Fig. 3C), which did not show surface light chain restriction. Rare scattered plump spindle cells were seen in the midst of the lymphoplasmacytic infiltrate. *IGH* gene rearrangement studies failed to show clonal rearrangement, while targeted RNA sequencing revealed an *ETV6-NTRK3* fusion. ALK-D5F3 IHC was negative in all three cases. Pan-TRK IHC was performed in two cases, revealing patchy nuclear positivity in the neoplastic cells in one case (Fig. 3D) and diffuse but weak nuclear positivity in the other. All patients were free of local recurrence of distant metastasis at 6, 13, and 1 months, respectively.

One case (IMT24, previously reported)[4] was characterized by *RET* rearrangement. This case occurred in a 27-year-old man with a 7.0 cm right upper lobe mass, which was surgically resected. Postoperative follow-up showed a 9.0 cm renal mass, which subsequently biopsied. The histologic findings from the lung primary and kidney metastases were morphologically similar, showing spindle cells arranged in herringbone architecture. The tumor cells showed mild to moderate cytologic atypia with 4 mitoses per 10 hpf. Unexpectedly, the tumor showed immunoreactivity for ALK IHC. The patient developed widespread metastases and died of disease 7 months later.

Combining the results from FISH and molecular testing, all thoracic IMTs were positive for kinase fusions or ATIs involving *ALK* (23 cases), *ROS1* (6 cases), *NTRK3* (3 cases), or *RET* (1 case).

DISCUSSION

Inflammatory myofibroblastic tumor (IMT) is currently classified as an intermediate, rarely metastasizing neoplasm composed of myofibroblasts accompanied by an inflammatory infiltrate composed of varying proportions of plasma cells, lymphocytes, and eosinophils. Most patients with IMT are children, adolescents, or young adults, although the tumor can occur throughout life[12]. Approximately 50–70% of the tumors harbor an *Anaplastic Lymphoma Kinase (ALK)* gene rearrangement, leading to the formation of a chimeric fusion protein, which is detectable by IHC or FISH[13, 14]. In IMT alone, more than 10 different genes have been identified as *ALK* fusion partners[14], which provide a strong promoter and an oligomerization domain, resulting in oncogenic activation of the ALK kinase.

Our study reveals that FISH testing can be reliably used to detect gene rearrangements, having a fast turn-around time, requiring minimal amount of tissue and a low cost. Overall, our results indicate that FISH analysis had a sensitivity of 86%, being positive in 26 of 30 cases with kinase rearrangements. Of the 4 cases negative by FISH, targeted RNA sequencing (Archer) detected *EML4-ALK* (n=2), *TMP4-ALK* (n=1), and *TFG-ROS1* (n=1). The two false negative cases harboring *EML4-ALK* fusion illustrated the challenges associated with the detection of intrachromosomal inversions inv(2)(p21p23) by FISH, due to the small and equivocal gaps present between the split probes. This has significant ramifications, since *EML4-ALK* is one of the most common fusion variants in thoracic IMTs compared to other anatomic sites[4]. Thus, a negative FISH result should not necessarily exclude a diagnosis of IMT in the setting of typical morphology, particularly when the tumor cells are positive for either ALK or ROS1 by IHC; in either situation, additional molecular testing such as Archer or other targeted RNA sequencing, is required to confirm the presence of fusion genes. The diagnostic utility of targeted RNA sequencing is highlighted by a subset of cases in which the abundance of lymphoplasmacytic infiltrate and relative paucity of spindle cells raised the differential diagnoses of IgG4-related disease and low-grade B-cell lymphoma. In these cases where the background inflammatory cells far outnumber the neoplastic spindle cells, targeted RNA sequencing generally shows greater analytical sensitivity than FISH due to fusions resulting in overexpression of mRNA transcript. In addition, accurate FISH scoring can be challenging in cases where the inflammatory infiltrate obscures the lesional cells, and the interpretation is dependent on the technical

expertise of the cytogenetic technologist. In laboratories without access to multiple FISH probes, in lieu of sequential IHC/FISH approach for diagnostic confirmation, the pathologist may consider moving directly to targeted RNA sequencing for a more expeditious approach. Given the morphologic overlap between IMT and its morphologic mimickers, many cases may require fusion testing as part of the diagnostic workup. In fact, we suspect that many of the so-called “plasma cell granulomas” reported in older literature may represent IMTs with modern ancillary diagnostic tools.

Our previous study investigating IMTs of all anatomic sites suggested that the prevalence of *ALK* gene rearrangements varies with age and anatomic site, with most of the fusion negative IMTs (90%) occurring in adults and outside the lung or soft tissue[4]. Our present results indeed confirm that using an array of complementary cytogenetic and molecular assays, most if not all thoracic IMT are characterized by fusions in *ALK* or other kinase genes.

Recent studies showed that *ALK* activation through alternative transcription initiation (*ALK*^{ATI}), a novel isoform of *ALK* transcript composed of a portion of *ALK* intron 19 followed by exons 20–29, are seen in approximately 11% of melanomas and sporadically in less than 1% of other malignancies, including non-small cell lung carcinoma, clear cell renal cell carcinoma, and invasive breast carcinoma[8]. *ALK*^{ATI} occurs independent of other genetic abnormalities, such as translocations or mutations of the *ALK* gene. *In vitro* and *in vivo* studies showed that patients with *ALK*^{ATI}-expressing tumors may benefit from ALK inhibitors[8]. To our knowledge, this is the first study documenting the presence of *ALK*^{ATI} as a driver event in IMTs and in tumors with intermediate malignant potential. As *ALK*^{ATI} results in increased nuclear and cytoplasmic localization of ALK protein, ALK IHC can be used as a screening tool for tumors harboring *ALK*^{ATI} [8]. While the initial study suggested that the detection of aberrant nuclear ALK IHC expression could be used as a biomarker to identify *ALK*^{ATI}-expressing tumors[8], the ALK IHC in the current case showed cytoplasmic positivity only. Therefore, nuclear localization of ALK protein expression may not be sufficiently sensitive as a surrogate marker for *ALK*^{ATI}. More importantly, the discrepancy between a positive ALK IHC and negative *ALK* FISH should prompt consideration of either a cryptic fusion undetectable by conventional FISH or alternatively *ALK*^{ATI}. Additional confirmatory studies such as NanoString can be utilized to investigate the presence of *ALK*^{ATI}. This may have therapeutic implications, as *ALK*^{ATI}-expressing tumors are predicted to show response to ALK inhibitors.

Our results show that *ROS1* gene fusion is the second most common abnormality detected in thoracic IMTs after *ALK* gene rearrangements. *ROS1*-related fusions also appear to be one of the most prevalent alterations in pediatric thoracic IMT, as a significant proportion of patients were 18 years old or younger. A previous study by Yamamoto et al.[15] found that 2 of 14 ALK-negative IMTs across all anatomic sites harbored *ROS1* fusions, and both cases from the study occurred in children. However, the diagnosis of ROS1-positive IMT may be challenging in this setting, since the tumor lacks ALK IHC expression, which might exclude a diagnosis of IMT, especially in a child. Furthermore, among the 6 cases with *ROS1* gene rearrangements, 1 (17%) case showed an unbalanced *ROS1* gene abnormality with deletion of centromeric signals, which was not diagnostic of gene rearrangement. In this case, ROS1

IHC positivity prompted further targeted RNA sequencing, revealing a *TFG-ROS1* fusion. The correct diagnosis is critical, since TKIs such as crizotinib are equally potent in tumors driven by either *ALK* or *ROS1* oncogenic fusions[16].

Six cases of *ETV6-NTRK3* positive IMTs have been so far reported in the literature, with 4 of 6 (67%) described in the lung, 1 in the liver, and the remaining 1 case in soft tissue[15, 17, 18]. Although *ETV6-NTRK3* fusions in mesenchymal neoplasms have been traditionally associated with pediatric tumors such as infantile fibrosarcoma and mesoblastic nephroma[12], IMTs harboring this gene fusion have a predilection for children and young adults with a median age of 17 years (range: 7 to 38 years). Our cohort had three *ETV6-NTRK3* positive IMTs from a 2-year-old child and two adults. *NTRK3*-rearranged IMTs showed a wide spectrum of morphology, ranging from tumors with myxoid features and scant inflammation to tumors with scant neoplastic cells obscured by exuberant plasmacytic infiltrate. Additionally, the latter case underscored the importance of fusion testing in confirming the histologic diagnosis, as the abundance of plasma cells raised the differential diagnosis of a hematopoietic neoplasm and IgG4-related disease. Interestingly, one of the patients had been treated with chemoradiation for lung adenocarcinoma, while the 2-year-old child had a history of adrenal neuroblastoma status post chemotherapy. As *TFE3* gene fusions have been documented in renal cell carcinomas in patients treated with chemotherapy for neuroblastoma[19, 20], the occurrence of *NTRK3* fusion positive IMTs in these 2 patients raises the question whether the *NTRK3* rearrangement arose as a therapy-related secondary event. Several preclinical and clinical studies have demonstrated that *ETV6-NTRK3* fusions are potentially targetable: previous reports demonstrated promising sensitivity to larotrectinib (LOXO-101), an inhibitor of TRK family, in *ETV6-NTRK3* fused infantile fibrosarcomas[21, 22].

In summary, our results show that despite a wide morphologic spectrum, thoracic IMTs were all characterized by an oncogenic activation of a tyrosine kinase protein, often through recurrent gene fusions and occasionally through an alternative mechanism not previously described in IMTs, *ALK*-alternative transcription initiation. We also show that one should not evaluate tumors only for *ALK* fusions: in FISH and IHC negative cases, it can be helpful to utilize targeted RNA sequencing to detect fusions including *ROS1* and *NTRK3*. Furthermore, in some cases where inflammatory or lymphoproliferative diagnoses are considered more likely on initial evaluation, documentation of gene fusions can be very helpful in confirming the diagnosis of IMT. These data not only provide insight into this rare tumor type but also offer rationale for targeted therapeutic strategies with existing FDA-approved TKIs based on the genomic profile of the tumor.

Supplementary Material

Refer to Web version on PubMed Central for supplementary material.

Acknowledgments

Supported in part by: P50 CA 140146–01 (CRA), P30 CA008748 (CRA), Cycle for Survival (CRA)

REFERENCES

1. Saab ST, Hornick JL, Fletcher CD, et al. IgG4 plasma cells in inflammatory myofibroblastic tumor: inflammatory marker or pathogenic link? Mod Pathol. 2011;24:606–612. [PubMed: 21297584]
2. Chan JK, Cheuk W, Shimizu M. Anaplastic lymphoma kinase expression in inflammatory pseudotumors. Am J Surg Pathol. 2001;25:761–768. [PubMed: 11395553]
3. Coffin CM, Patel A, Perkins S, et al. ALK1 and p80 expression and chromosomal rearrangements involving 2p23 in inflammatory myofibroblastic tumor. Mod Pathol. 2001;14:569–576. [PubMed: 11406658]
4. Antonescu CR, Suurmeijer AJ, Zhang L, et al. Molecular characterization of inflammatory myofibroblastic tumors with frequent ALK and ROS1 gene fusions and rare novel RET rearrangement. Am J Surg Pathol. 2015;39:957–967. [PubMed: 25723109]
5. Kao YC, Fletcher CDM, Alaggio R, et al. Recurrent BRAF Gene Fusions in a Subset of Pediatric Spindle Cell Sarcomas: Expanding the Genetic Spectrum of Tumors With Overlapping Features With Infantile Fibrosarcoma. Am J Surg Pathol. 2018;42:28–38. [PubMed: 28877062]
6. Zheng Z, Liebers M, Zhelyazkova B, et al. Anchored multiplex PCR for targeted next-generation sequencing. Nature medicine. 2014;20:1479–1484.
7. Geiss GK, Bumgarner RE, Birditt B, et al. Direct multiplexed measurement of gene expression with color-coded probe pairs. Nature biotechnology. 2008;26:317–325.
8. Wiesner T, Lee W, Obenauf AC, et al. Alternative transcription initiation leads to expression of a novel ALK isoform in cancer. Nature. 2015;526:453–457. [PubMed: 26444240]
9. Reis PP, Waldron L, Goswami RS, et al. mRNA transcript quantification in archival samples using multiplexed, color-coded probes. BMC biotechnology. 2011;11:46. [PubMed: 21549012]
10. Kadota K, Suzuki K, Kachala SS, et al. A grading system combining architectural features and mitotic count predicts recurrence in stage I lung adenocarcinoma. Mod Pathol. 2012;25:1117–1127. [PubMed: 22499226]
11. Marino-Enriquez A, Wang WL, Roy A, et al. Epithelioid inflammatory myofibroblastic sarcoma: An aggressive intra-abdominal variant of inflammatory myofibroblastic tumor with nuclear membrane or perinuclear ALK. Am J Surg Pathol. 2011;35:135–144. [PubMed: 21164297]
12. Fletcher CDM, Bridge JA, Hogendoorn P, Mertens F WHO Classification of Tumours of Soft Tissue and Bone. IARC Press; 2013.
13. Griffin CA, Hawkins AL, Dvorak C, et al. Recurrent involvement of 2p23 in inflammatory myofibroblastic tumors. Cancer Res. 1999;59:2776–2780. [PubMed: 10383129]
14. Lovly CM, Gupta A, Lipson D, et al. Inflammatory myofibroblastic tumors harbor multiple potentially actionable kinase fusions. Cancer discovery. 2014;4:889–895. [PubMed: 24875859]
15. Yamamoto HYA, Taguchi K, Kohashi K, Hatanaka Y, Yamashita A, Mori D, Oda Y. ALK, ROS1 and NTRK3 gene rearrangements in inflammatory myofibroblastic tumours. Histopathology. 2016;69:72–83. [PubMed: 26647767]
16. Shaw AT, Ou S-HI, Bang Y-J, et al. Crizotinib in ROS1-Rearranged Non–Small-Cell Lung Cancer. New England Journal of Medicine. 2014;371:1963–1971. [PubMed: 25264305]
17. Alassiri AH, Ali RH, Shen Y, et al. ETV6-NTRK3 Is Expressed in a Subset of ALK-Negative Inflammatory Myofibroblastic Tumors. Am J Surg Pathol. 2016;40:1051–1061. [PubMed: 27259007]
18. Pavlick D, Schrock AB, Malicki D, et al. Identification of NTRK fusions in pediatric mesenchymal tumors. Pediatric blood & cancer. 2017;64. [PubMed: 27555087]
19. Calió A, Grignon DJ, Stohr BA, et al. Renal cell carcinoma with TFE3 translocation and succinate dehydrogenase B mutation. Modern Pathology. 2016;30:407. [PubMed: 27910947]
20. Falzarano SM, McKenney JK, Montironi R, et al. Renal Cell Carcinoma Occurring in Patients With Prior Neuroblastoma: A Heterogenous Group of Neoplasms. The American Journal of Surgical Pathology. 2016;40:989–997. [PubMed: 26975037]
21. Nagasubramanian R, Wei J, Gordon P, et al. Infantile Fibrosarcoma With NTRK3-ETV6 Fusion Successfully Treated With the Tropomyosin-Related Kinase Inhibitor LOXO-101. Pediatric blood & cancer. 2016;63:1468–1470. [PubMed: 27093299]

22. Drilon A, Laetsch TW, Kummar S, et al. Efficacy of Larotrectinib in TRK Fusion–Positive Cancers in Adults and Children. New England Journal of Medicine. 2018;378:731–739. [PubMed: 29466156]

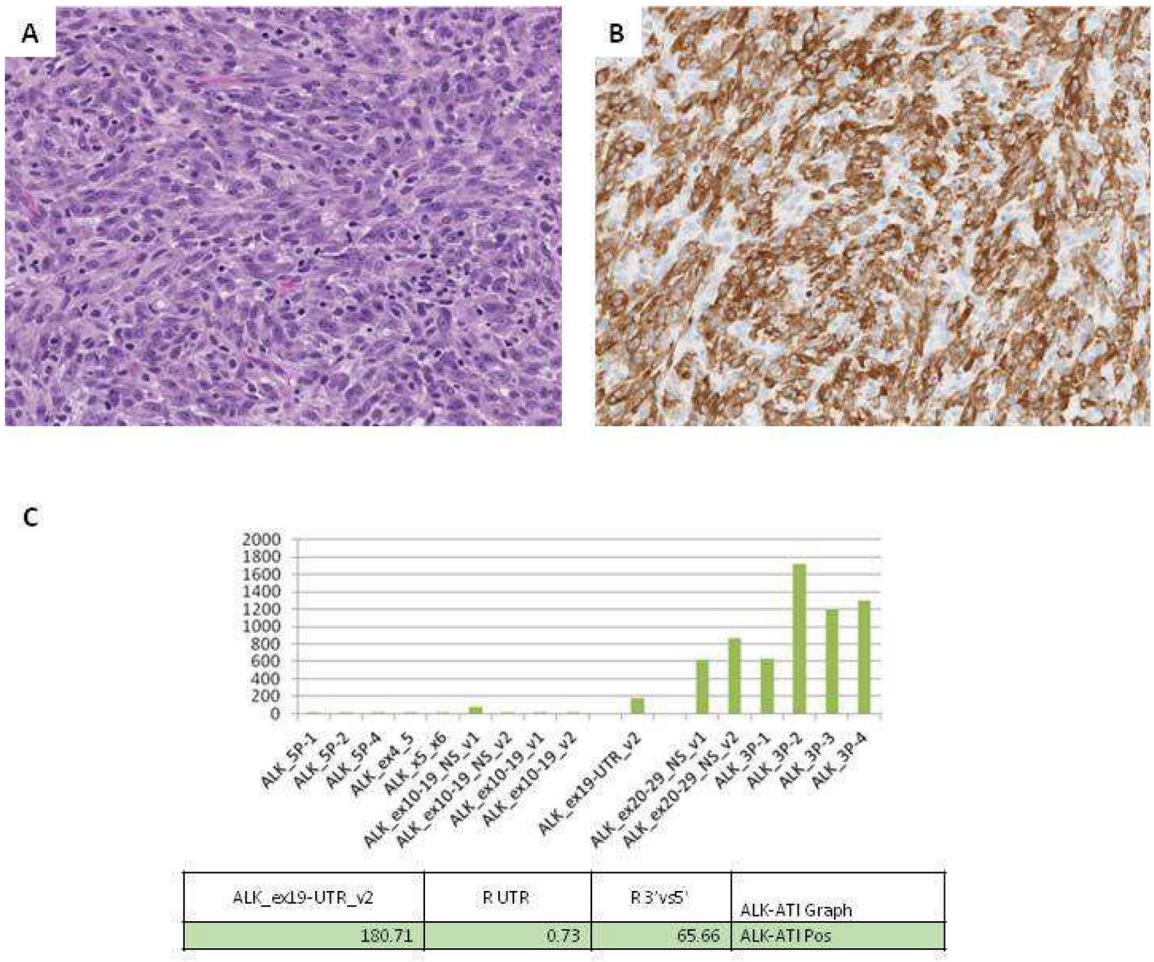

Figure 1. Pulmonary IMT with novel *ALK*^{ATI} (IMT23).

A, Relatively monomorphic plump spindle cell proliferation arranged in short fascicule and vague storiform pattern and scattered inflammatory infiltrate. B, ALK IHC shows diffuse cytoplasmic positivity. C, NanoString assay shows overexpression of *ALK* intron 19 and exons 20–29 relative to exons 1–19, in keeping with presence of *ALK*$^{ATI.}$

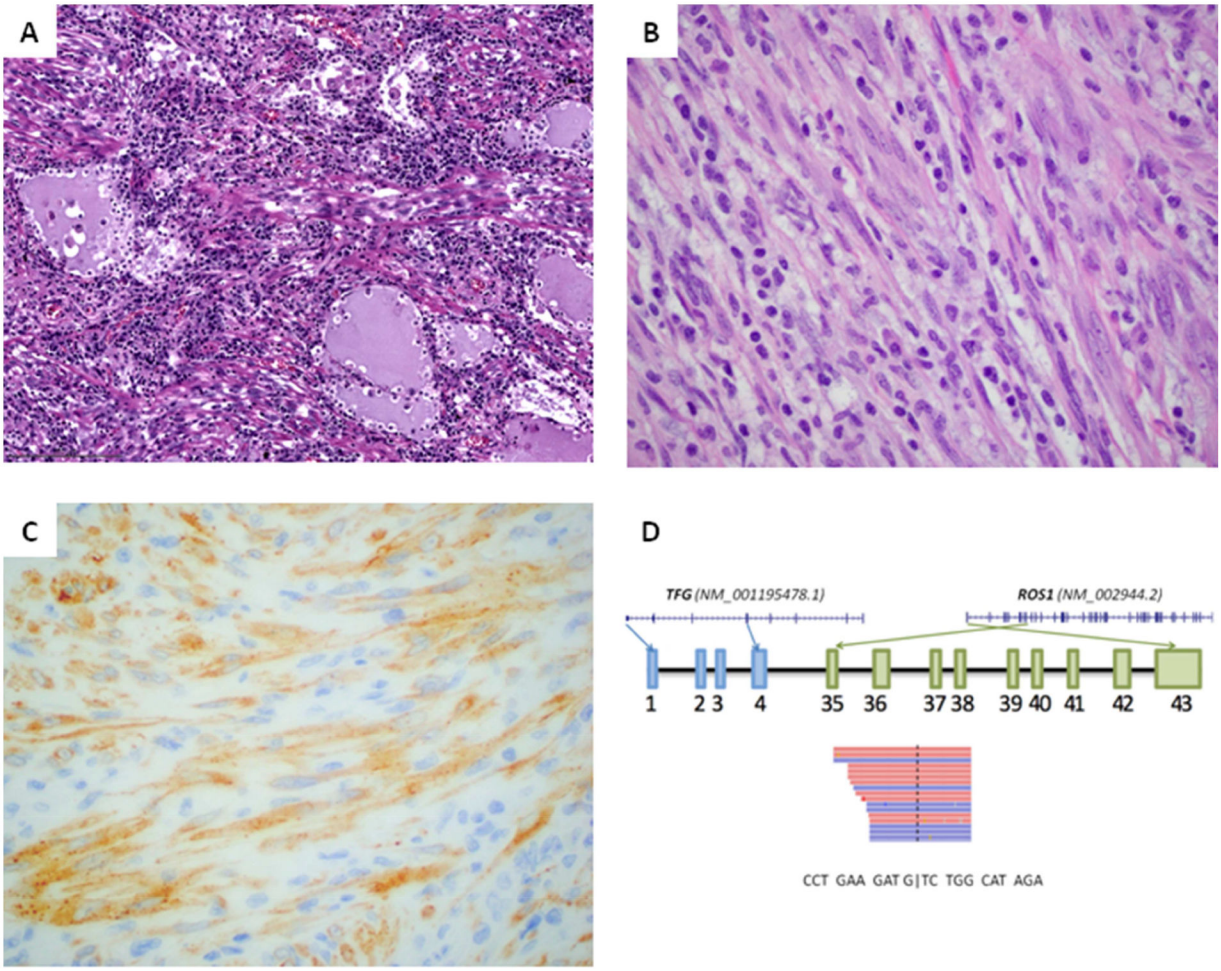

Figure 2. Histologic and molecular findings of *ROS1*-rearranged pulmonary IMTs.

A, A peculiar case of IMT showing cellular expansion of interstitium entrapping native alveolar parenchyma. B, Most cases show a spindle cell proliferation with distinctive slender cytoplasmic processes arranged in loose fascicles with variably abundant inflammatory infiltrate (IMT27). B, ROS1 IHC shows diffuse cytoplasmic positivity (IMT28). C, Schematic illustration of the gene structure and transcript sequence of the *TFG-ROS1* fusion product and representation of cDNA sequencing reads supporting the fusion transcript by targeted RNA sequencing (IMT28).

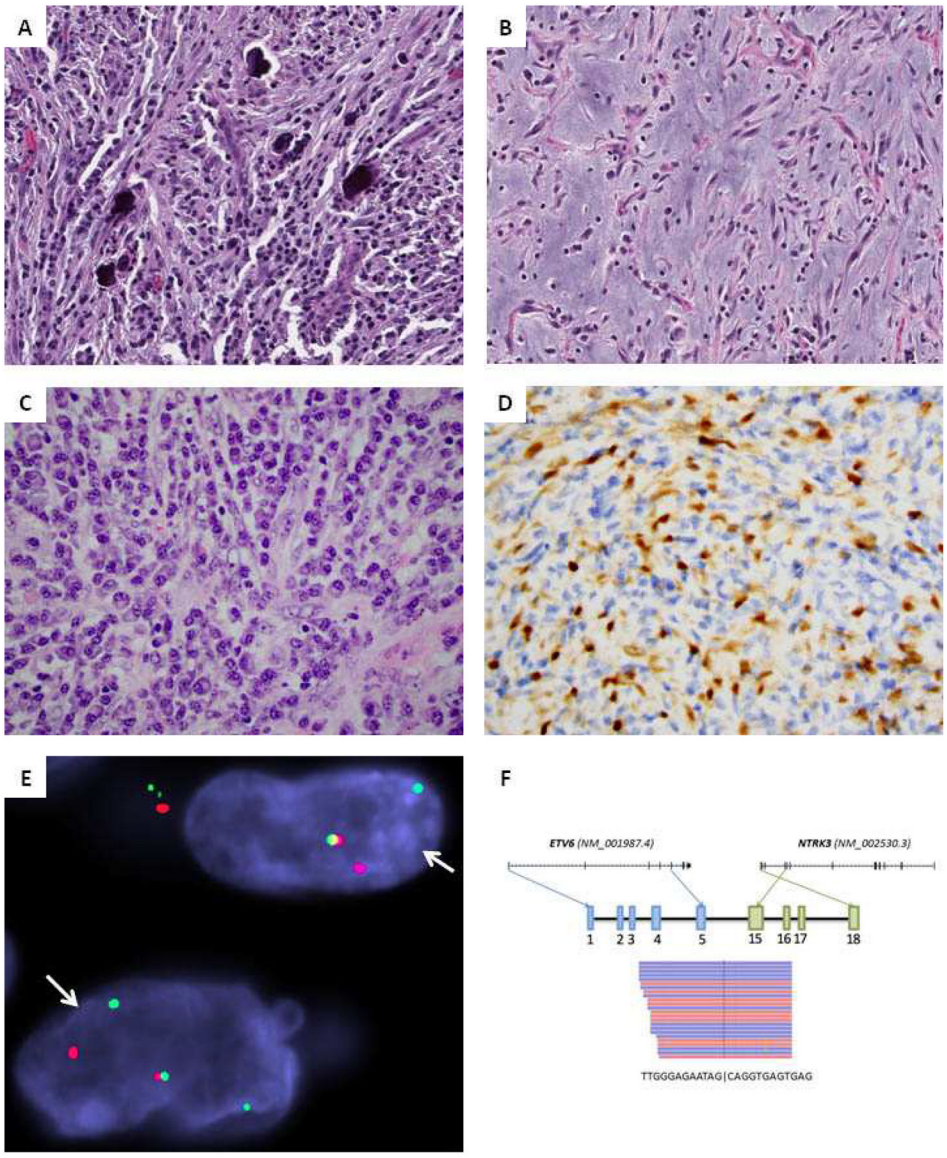

Figure 3. Histologic and molecular findings of *NTRK3*-rearranged pulmonary IMTs.

A, Vaguely fascicular growth of spindle cells with abundant lymphoplasmacytic infiltrate and numerous psammomatous calcifications (IMT32). B, Scattered spindle cells embedded in abundant myxoid stroma and scant inflammation (IMT31). C, Rare plump spindle cells surrounded by exuberant chronic inflammatory infiltrate rich in plasma cells (IMT33). D, Pan-TRK IHC shows patchy cytoplasmic positivity in the lesional cells (IMT32). E, FISH assay shows rearrangement of *NTRK3* gene, with break-apart of centrometric (red) and telomeric (green) signals. F, Schematic illustration of the gene structure and transcript sequence of the *ETV6-NTRK3* fusion product and representation of cDNA sequencing reads supporting the fusion transcript by targeted RNA sequencing (IMT32).

J Thorac Oncol. Author manuscript; available in PMC 2020 May 01.

Table 1

Clinical, IHC, FISH, and molecular findings in pulmonary IMTs

IMT	Age/Sex	Location	Size (cm)	ALK IHC	FISH results	RNA-seq results	Driver summary	Histologic findings (cell shape, architecture, cytologic atypia, mitosis)
IMT1	14/M	LUL	NA	Pos	ALK pos	ND	*ALK* fusion	Spindle cells, fascicular, none, 4/10
IMT2	23/F	LUL	3.5	Pos	ALK pos	ND	*ALK* fusion	Spindle cells, fascicular and storiform, mild, 1/10
IMT3	6/F	RUL	4.6	Pos	ALK pos	ND	*ALK* fusion	Spindle/epithelioid, fascicular, mild, 2/10
IMT4	24/F	RUL	NA	Pos	ALK pos	ND	*ALK* fusion	Spindle cells, fascicular and storiform, none, 2/10
IMT5	52/M	LUL	NA	Pos	ALK pos	ND	*ALK* fusion	Spindle/epithelioid, fascicular and storiform, mild, 1/10
IMT6	19/F	RUL	NA	Pos	ALK pos	ND	*ALK* fusion	Spindle cells, fascicular, mild, <1/10
IMT7	39/F	LLL	NA	Pos	ALK pos	ND	*ALK* fusion	Spindle cells, fascicular, none, 1/10
IMT8	60/F	RLL	3.6	Pos	ALK pos	ND	*ALK* fusion	Spindle/epithelioid, patternless, moderate to severe, 3/10
IMT9	70/F	L pleural bx	NA	Pos	ALK pos	ND	*ALK* fusion	Epithelioid, solid, mild, 15/10
IMT10	40/F	LLL	15.4	Pos	ALK pos	ND	*ALK* fusion	Spindle/epithelioid, fascicular, mild to focally moderate, 9/10
IMT11	20/F	RML	3.2	Pos	ALK pos	ND	*ALK* fusion	Spindle cells, fascicular and storiform, mild, 2/10
IMT12	42/F	RUL	1.5	Pos	ALK pos	ND	*ALK* fusion	Spindle cells, fascicular and storiform, none, <1/10
IMT13	46/M	LUL	1.4	Pos	ALK pos	ND	*ALK* fusion	Spindle cells, fascicular and storiform, none, 2/10
IMT14	67/F	RUL	1.5	Pos	ALK pos	ND	*ALK* fusion	Spindle cells, fascicular, mild, 1/10
IMT15	37/F	LLL	2.7	Pos	ALK pos	ND	*ALK* fusion	Spindle cells, fascicular and storiform, mild, <1/10
IMT16	41/F	RUL	1.2	Pos	ALK pos	ND	*ALK* fusion	Spindle cells, fascicular and storiform, mild, 1/10
IMT17	29/F	L bronchus	2.3	Pos	ALK pos	ND	*ALK* fusion	Spindle cells, fascicular and storiform, none, 2/10
IMT18	37/F	LUL	4.0	Pos	ALK pos	ND	*ALK* fusion	Spindle cells, fascicular and storiform, none, 2/10
IMT19	18/F	Lung	NA	Pos	ALK pos	ND	*ALK fusion*	Spindle cells, fascicular, mild, 1/10
IMT20	59/F	RLL	2.0	Pos	ALK neg	*TMP4-ALK*	*ALK* fusion	Spindle/epithelioid, fascicular and storiform, none, 1/10
IMT21	41/F	Left lung bx	NA	Pos	ALK neg	*EML4-ALK*	*ALK* fusion	Spindle cells, fascicular and storiform, mild, 1/10
IMT22	40/F	RUL	2.6	Pos	ALK neg	*EML4-ALK*	*ALK* fusion	Spindle cells, fascicular and storiform, mild, <1/10
IMT23	40/M	R bronchus	1.8	Pos	ALK neg	ALK^{ATI}	ALK^{ATI}	Spindle cells, vague storiform, mild, 4/10
IMT24	27/M	Lung	NA	Pos	ALK neg/RET pos	ND	*RET* fusion	Spindle cells, fascicular, mild, 4/10
IMT25	18/M	Mediastinum	NA	Neg	ALK neg/ROS1 pos	ND	*ROS1* fusion	Spindle cells, vague storiform, none, <1/10
IMT26	7/M	Right lung	11.7	Neg	ALK neg/ROS1 pos	ND	*ROS1* fusion	Spindle cells, fascicular, none, 1/10

IMT	Age/Sex	Location	Size (cm)	ALK IHC	FISH results	RNA-seq results	Driver summary	Histologic findings (cell shape, architecture, cytologic atypia, mitosis)
IMT27	75/F	LUL	1.0	Neg	ALK neg/ROS1 pos	ND	*ROS1* fusion	Spindle cells, fascicular, mild, <1/10
IMT28	10/F	Left lung bx	NA	Neg	ALK neg/ROS1 neg/NTRK3 neg	*TFG-ROS1*	*ROS1* fusion	Spindle cells, vaguely fascicular, mild, <1/10
IMT29	32/F	LLL	4.9	Neg	ND	*TFG-ROS1*	*ROS1* fusion	Spindle cells, vaguely fascicular, none, <1/10
IMT30	20/F	LLL	6.0	Neg	ALK neg/ROS1 pos	ND	*ROS1* fusion	Spindle cells, vaguely fascicular, none, <1/10
IMT31	31/F	RLL	1.8	Neg	ALK neg/NTRK3 pos/ETV6 pos	ND	*NTRK3* fusion	Spindle cells, fascicular and storiform, mild, 1/10
IMT32	2/M	RLL	1.2	Neg	ALK neg/NTRK3 pos/ETV6 pos	*ETV6-NTRK3*	*NTRK3* fusion	Spindle cells, fascicular, mild, <1/10
IMT33	61/F	LUL	1.1	Neg	ND	*ETV6-NTRK3*	*NTRK3* fusion	Spindle cells, vaguely fascicular, mild to moderate, 1/10

Bx – biopsy; LUL – left upper lobe; LLL – left lower lobe; RUL – right upper lobe; RML – right middle lobe; RLL – right lower lobe; NA – not available; ND – not done